JOURNAL OF GEOPHYSICAL RESEARCH, VOL. 113, D17309, doi:10.1029/2007JD009443, 2008

Seasonal CO_2 rectifier effect and large-scale extratropical atmospheric transport

Douglas Chan,[1] Misa Ishizawa,[1,2] Kaz Higuchi,[1] Shamil Maksyutov,[3] and Jing Chen[2]

Received 1 October 2007; revised 19 February 2008; accepted 23 June 2008; published 9 September 2008.

[1] In atmospheric transport models, the covariation of the atmospheric transport and annually neutral biospheric CO_2 flux is usually evident as the annual zonal mean surface CO_2 concentration gradient. Using the NIES transport model and CO_2 flux from the Biome-BGC model, the covariations of different transport mechanisms and CO_2 flux were examined and quantified. Including the covariation of the total transport (processes included in the NIES model) and CO_2 flux, the annual average pole to pole CO_2 concentration gradient is 3.5 ppm and interhemispheric difference of the average extratropical surface concentration is 2.5 ppm. The conventional covariation mechanism of the seasonal variation of planetary boundary layer mixing height and CO_2 flux accounts for approximately 45% of the CO_2 concentration gradient. Another important contribution to the CO_2 concentration gradient in this model is the covariation of the extratropical anomaly transport (mainly by cyclones and anticyclones) and the biospheric flux, which accounts for about 55%. This alternate physical mechanism is the association of stronger meridional (north–south) anomaly transport (under strong baroclinic instability condition) with higher CO_2 concentration from soil respiration in the winter and weaker anomaly transport (weak baroclinic instability condition) with lower CO_2 concentration from photosynthetic uptake in the summer. The net result of the meridional transport and flux covariation is a north–south annual zonal mean CO_2 concentration gradient.

Citation: Chan, D., M. Ishizawa, K. Higuchi, S. Maksyutov, and J. Chen (2008), Seasonal CO_2 rectifier effect and large-scale extratropical atmospheric transport, *J. Geophys. Res.*, *113*, D17309, doi:10.1029/2007JD009443.

1. Introduction

[2] Inverse modeling is a procedure used to estimate sources and sinks of CO_2 using atmospheric CO_2 concentration measurements. To compensate for the sparseness of CO_2 concentration observations, inverse models typically employ constraining conditions. One common constraint is the specification of the "background" CO_2 fluxes from fossil fuel, ocean, and seasonal terrestrial biosphere [e.g., *Fan et al.*, 1998; *Gurney et al.*, 2002; *Baker et al.*, 2006] to generate the "background" CO_2 concentration in atmospheric transport models. In this type of inversion procedure, the inversion flux estimates are sensitive to the errors in the simulated "background" CO_2 concentration [*Denning et al.*, 1995; *Gurney et al.*, 2002].

[3] A part of the CO_2 background distribution is produced by the biospheric fluxes. Using atmospheric circulation models and specified annually neutral (no net flux on an annual basis) biospheric fluxes, the resultant annual mean surface CO_2 distribution in the atmosphere is often nonuniform [*Denning et al.*, 1995; *Gurney et al.*, 2003]. This annual mean surface CO_2 distribution, generally referred to as the rectifier effect, is the result of the covariation of the atmospheric transport and biospheric flux. The term "covariation of atmospheric transport and flux" indicates the time variation of atmospheric transport (wind and the model parameterization of the subgrid scale wind fluctuations) is accompanied by the time variation of CO_2 flux input into the bottom layer of an atmospheric model (becoming CO_2 concentration and then subsequently transported to other atmospheric regions). This terminology avoids the possible confusion that CO_2 flux is only applied at the surface of an atmospheric transport model where velocity or transport technically vanishes and the "covariance of transport and flux" would also vanish. In general, the covariation of "a" and "b" refers to the simultaneous variations in both "a" and "b".

[4] The annual mean CO_2 distribution resulting from a neutral biosphere typically shows a north–south gradient with higher CO_2 concentration near the northern polar region than the tropics and Southern Hemisphere. This mean annual north–south gradient in the CO_2 concentration distribution is an important feature as it has implication on the spatial distribution of the CO_2 sources and sinks and consequently this feature has also been referred to as the rectifier effect [*Denning et al.*, 1999]. The term "rectifier effect" has acquired several meanings; however, the meaning in each case can usually be inferred by its usage.

[1] Atmosheric Science and Technology Directorate, Environment Canada, Toronto, Ontario, Canada.
[2] Department of Geography, University of Toronto, Toronto, Ontario, Canada.
[3] National Institute for Environmental Studies, Tsukuba, Japan.

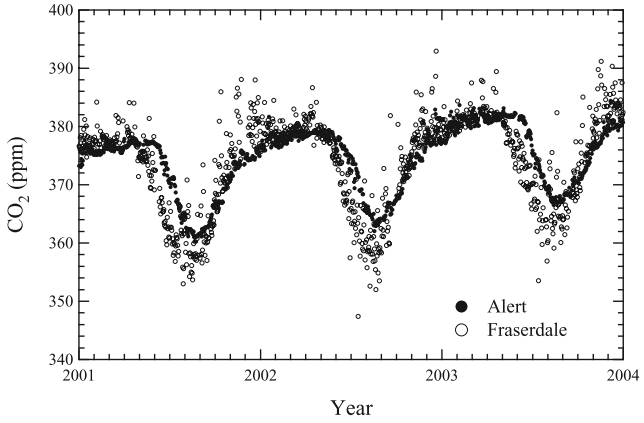

Figure 1. Daily CO_2 concentration time series at Fraserdale (50°N, 81°W) and Alert (82°N, 62°W) in ppm, from 2001 to 2003.

[5] It has been postulated that the main physical mechanism of the rectifier effect (the physical mechanism is sometimes referred to as rectifier forcing) is the covariation of the biospheric flux and the vertical mixing in the planetary boundary layer (PBL), the simultaneous variation of vertical mixing in the PBL and biospheric flux (summer photosynthetic uptake and vertical mixing in a deep PBL compared to winter ecosystem respiratory release and vertical mixing in a shallow PBL). However the covariation between the biospheric CO_2 flux and the vertical mixing in the PBL is insufficient to explain all the rectifier effect results in model simulations. An indication of the importance of other mechanism(s) can be seen in the presence of the rectifier effect in atmospheric transport models with no PBL variation. Some examples are the Japan Meteorological Agency (JMA) model [*Gurney et al.*, 2005] and in a sensitivity case study for the National Institute for Resources and Environment (NIRE) model (reported in *Taguchi* [1996]).

[6] Observational evidence also provides some hints of other physical mechanism(s). Figure 1 shows the daily CO_2 concentration time series at Fraserdale (50°N, 81°W) and Alert (82°N, 62°W). Fraserdale is a continental site situated in the North American boreal forest with black spruce being the dominant species [*Higuchi et al.*, 2003; *Worthy et al.*, 2003]. Alert is the northernmost background monitoring site in the Global Atmospheric Watch (GAW) network [*Trivett and Higuchi*, 1989; *Worthy et al.*, 2003]. The CO_2 concentration at Fraserdale is taken from the afternoon average (from 15:00 to 18:00 local time) as a representation of the average concentration in the fully developed PBL and to minimize the interference from the large diurnal cycle typically observed at continental sites. The figure shows a large concentration difference between Fraserdale and Alert throughout the northern midlatitude growing season from May to September (lower at Fraserdale than at Alert) and a small concentration difference from October to April.

[7] The main causal source of the observed atmospheric CO_2 seasonal cycle at various locations in the world is the seasonal variation in the net biospheric CO_2 flux and the subsequent atmospheric transport. Fraserdale is surrounded by strong biospheric sources and sinks, the seasonal cycle amplitude is therefore larger than at Alert and represents CO_2 concentration at the source/sink region. Since there is no significant biospheric flux in the northern polar region, the CO_2 seasonal cycle at Alert is mostly a result of atmospheric transport from the dominant biospheric flux regions in the northern midlatitudes. The differences in the CO_2 seasonal cycle between Fraserdale and Alert suggest that the transport is changing with the seasons: The small CO_2 difference or gradient in the winter between these stations suggests a strong meridional (north–south) advective transport, and the large CO_2 gradient in the summer suggests a weak meridional advective transport. The apparently weak meridional transport in the Northern Hemisphere summer of the low CO_2 concentration (from plant photosynthesis) and the strong meridional transport in the winter of the high CO_2 concentration (from soil respiration) imply high CO_2 concentration air is preferentially transported to the polar region. This mechanism of seasonal meridional transport-flux covariation has the characteristics of a north–south rectifier (rectifier refers to the physical mechanism of preferential or enhanced northward movement of high CO_2 concentration air over low CO_2 concentration air), as opposed to the seasonal PBL mixing-flux covariation which acts vertically. Thus PBL mixing-flux covariation acts locally over the PBL column, while transport-flux covariation propagates inherently. PBL-flux covariation can be considered a subset of the atmospheric transport-flux covariation.

[8] *Denning et al.* [1999] noted that typical synthesis inversion estimates are sensitive to the annual mean background biospheric CO_2 distribution in the atmosphere. This background is explicitly included in some annual mean inversions [e.g., *Gurney et al.*, 2003], and implicitly in some seasonal inversion [e.g., *Gurney et al.*, 2004] and inter-annual inversion [e.g., *Baker et al.*, 2006], through the corresponding monthly biospheric background CO_2 distribution. Hence the understanding of this atmosphere-biosphere interaction is important to determine if the model is correctly simulating this interaction. Some previous studies have investigated the rectifier effect by examining different parameterizations or models: *Taguchi* [1996] examined the role of different PBL parameterization schemes, *Law and Rayner* [1999] compared two atmospheric transport models with different parameterization of subgrid scale vertical diffusion and the relative contribution of horizontal and vertical transport, *Taylor* [1998] studied the relative contributions of vertical and horizontal transport at a point with a box model. *Dargaville et al.* [2003] commented on the vertical versus horizontal contributions to the rectifier. *Gurney et al.* [2003] compared the rectifier effects in different atmospheric transport models, and *Engelen et al.* [2002] considered the rectifier effects of different biospheric flux models.

[9] There are also experimental studies of the rectifier forcing including aircraft measurements [e.g., *Lin et al.*, 2004; *Gerbig et al.*, 2006], tower measurements, and radar PBL profiling [e.g., *Yi et al.*, 2001, 2004; *Bakwin et al.*, 2004; *Hurwitz et al.*, 2004].

[10] In this study, the different components of atmospheric transport will be examined. We will use an atmospheric transport model and a biospheric flux model in a series of sensitivity experiments to estimate the contributions of the

various horizontal and vertical transport mechanisms on the atmospheric CO_2 distribution. Examining different transport mechanisms in the same atmospheric model eliminates the complication of comparing rectification in inherently different transport models [e.g., *Gurney et al.*, 2003].

2. Method

[11] In this study, the covariations of different atmospheric transport mechanisms and biospheric CO_2 fluxes are investigated using the National Institute for Environmental Studies (NIES) transport model [*Maksyutov and Inoue*, 2000] and the annually neutral biospheric flux from the Biome-BGC (bio-geochemical cycle) model [*Thornton et al.*, 2002; *Fujita et al.*, 2003]. This model combination has been used in the CO_2 inversion studies of *Ishizawa et al.* [2006] and *Deng et al.* [2007].

[12] Briefly, the NIES model has horizontal resolution of $2.5^\circ \times 2.5^\circ$ in latitude and longitude. Vertically, the model has 15 σ levels ($\sigma = p/p_0$, the ratio of pressure to surface pressure) ranging from 0.985 to 0.065 ($\sim$0.15 km to $\sim$20 km in altitude, exact height depends on surface pressure). Time step in the model is 2 hours. The advection scheme is semi-Lagrangian with mass adjustment to conserve tracer mass. The wind field used is the NCEP (National Centers for Environmental Prediction) reanalysis [*Kalnay et al.*, 1996] with $2.5^\circ \times 2.5^\circ$ horizontal resolution and 12-hourly time resolution (wind is linearly interpolated to the 2 hourly model time step). The seasonal variation of the PBL height at each grid point in the model is specified with the monthly mean climatological heights (from the Data Assimilation Office at NASA's Goddard Space Flight Center). Note that *Taguchi* [1996] found a large sensitivity to whether monthly mean or 6 hourly PBL heights were used in his model. The well-mixed state in the PBL is accomplished with the spatiotemporally constant turbulent diffusion coefficient set to 40 $m^2\ s^{-1}$. Other vertical mixing processes in the model are (1) turbulent diffusion as a function of vertical temperature stability and (2) cumulus convection derived from the humidity, temperature, and wind fields obtained from the NCEP reanalysis data (see Appendix A in *Ishizawa et al.* [2006]). As a result of the model resolution, transport processes on the mesoscale or shorter space and timescales are not included.

[13] The Biome-BGC model is a biospheric process-based model that computes the daily ecosystem fluxes, including net primary production (NPP), heterotrophic respiration (HR), and net ecosystem exchange (NEE = NPP+HR) as a function of atmospheric temperature, humidity, precipitation, and radiation. The model resolution is $1^\circ \times 1^\circ$ in latitude and longitude, and the time step is 1 day. The meteorological forcing is the NCEP reanalysis meteorology linearly interpolated from the T63 Gaussian domain (192 grids in longitude, 94 in latitude with a Gaussian distribution). The global biospheric fluxes of NPP and HR are simulated with the Biome-BGC model and the NCEP meteorology for the 10-year period from 1990 to 1999. The net flux of NPP and HR (or NEE) is then adjusted to be annually neutral (zero annual total) at every grid point for each year. The adjustment consists of applying a small constant correction term to NEE throughout the year. The annually balanced or neutral NEE flux is further averaged for each individual month over the 10 years to give the mean monthly NEE fluxes. This mean monthly NEE flux is comparable to the CASA (Carnegie-Ames Stanford Approach) NEE flux [*Randerson et al.*, 1997,] used in the TransCom 3 (Atmospheric Tracer Transport Model Intercomparison Project) experiments [*Gurney et al.*, 2000].

[14] A series of experiments examining different atmospheric transport processes in the NIES transport model were done. The differences among these experiments are explained in the next section. Each experiment consists of a 10-year model simulation using NCEP winds from 1990 to 1999 and the monthly mean NEE flux repeated each year. The first 2 years of each simulation were considered model spin up, then the surface CO_2 concentrations for the final 8 years of simulations were averaged to represent the model annual mean. The mean simulated CO_2 concentration at the South Pole for each experiment serves as the reference CO_2 concentration in the presentation of the model results, it is defined as 0 ppm (in this study, ppm denotes parts per million by volume). The results presented will focus mainly on the annual zonal mean surface CO_2 concentration following previous studies on the rectifier effect.

3. Results and Discussion

[15] Before presenting the results, a brief discussion of the factors governing the atmospheric transport may be helpful in understanding the results. The spherical geometry of the earth results in the differential solar heating between the tropics and the polar regions. The atmosphere transfers the heat from the tropics to the polar regions along the thermal gradient; this energy transfer provides the main driving force for the atmospheric general circulation.

[16] In the tropics, the mean meridional circulation is represented by the Hadley circulation [*Peixoto and Oort*, 1992]. The Hadley circulation is classified as thermally direct, with warm air rising in the equatorial region, moves poleward in the upper troposphere, cools and sinks near 30° latitudes. In the extratropics, the mean circulation is the Ferrell circulation. The Ferrell circulation is a weak circulation since it is thermally indirect. In the Northern Hemisphere, for example, the sinking of warm air occurs in the south (near 30°N), while the rising of cooler air occurs in the north (near 60°N but varies greatly). The more dominant transport mechanism in the extratropics is the instability-driven anomalies or eddies. The horizontal temperature gradient from the tropics to the polar region is thermodynamically unstable, resulting in baroclinic instability [see, for example, *Holton*, 2004]. Typically, the fastest growing mode of baroclinic instability results in the formation of synoptic scale eddies of cyclones and anticyclones, collectively called large-scale eddies (LSE). Large-scale eddies have horizontal length scale of $\sim$1000 km, vertical length scale of $\sim$10 km and temporal scale of $\sim$10 days.

[17] Meridionally, the strength of the LSE transport is proportional to the horizontal temperature gradient $\partial T/\partial y$ [*Green*, 1970; *Stone*, 1974]. In the Northern Hemisphere, there are large seasonal variations in the horizontal temperature gradient. In the summer, the average equator to pole temperature difference is $\sim$20°C; while the winter average equator to pole temperature difference is $\sim$40°C [*Peixoto and Oort*, 1992]. Thus the meridional transport in the winter

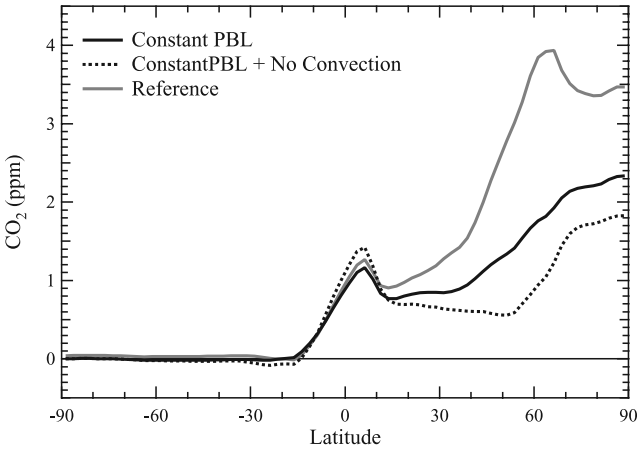

Figure 2. Latitudinal distributions of annual zonal mean surface CO_2 concentrations (in ppm) for three experimental cases: (1) reference experiment, (2) experiment with constant PBL (each grid point specified with its annual mean PBL height), and (3) experiment with constant PBL and convective adjustment in the transport model turned off.

season is about twice as strong as the summer transport. In combination with the seasonal variation of the biospheric CO_2 fluxes predominantly from the midlatitudes of the Northern Hemisphere, the covariation of the seasonal LSE transport with the biospheric CO_2 fluxes results in strong meridional transport to the northern high latitudes of the high CO_2 concentration air (from fall and winter respiration in the northern midlatitude region) and weak meridional transport of low CO_2 concentration air (from summer photosynthesis). This process should yield higher CO_2 concentration in the annual average in the northern high latitudes, resulting in an annual mean CO_2 gradient between the northern polar region and the tropics.

3.1. Reference Case

[18] As a basis for comparison, the reference case was constructed in which the input of CO_2 into the atmospheric transport model is driven by the monthly averaged CO_2 flux from the Biome-BGC model. In this reference case experiment, the PBL in the transport model is prescribed with the monthly average PBL height. The annual zonal mean (averaged over 8 years) CO_2 concentration at the surface is shown in Figure 2.

[19] The covariation of the transport and CO_2 flux results in higher CO_2 concentration ($\sim$3.5 ppm) in the northern polar region, with the concentration gradually decreasing to zero at 20°S, a pole to pole concentration difference of 3.5 ppm. Another commonly used measure of the concentration gradient is the interhemispheric difference (the Northern Hemisphere average surface CO_2 concentration minus the Southern Hemisphere average surface CO_2 concentration). Since the covariation of LSE transport and biospheric flux and the covariation of PBL mixing and biospheric flux are essentially extra-tropical processes, we define a similar measure to focus on the extra-tropical region, the interhemispheric extra-tropical difference (IHED) (the extra-tropical Northern Hemisphere average surface CO_2 concentration from 30°N to 90°N minus the extra-tropical Southern Hemisphere average surface CO_2 concentration from 30°S to 90°S). The IHED for the reference case is 2.5 ppm. The pole to pole concentration difference is more representative of the marine boundary layer condition, and the IHED includes the continental biospheric source regions. This reference CO_2 distribution is comparable to the results of other models in the TransCom studies [*Gurney et al.*, 2003]; it represents the covariation of the total transport (as represented in this model) and the biospheric flux and will be included in subsequent plots of model experiments for comparison. The spatial distribution of the annual mean surface CO_2 concentration will be presented in section 3.3 in a comparison with the other simulations. The following sections will examine how different components of the transport-flux covariation affect the north–south annual mean zonal gradient of atmospheric CO_2.

3.2. Constant PBL Case

[20] To quantify the importance of the covariation of PBL height and the CO_2 flux in the north–south annual mean zonal gradient of atmospheric CO_2, a simulation is performed with a constant PBL height distribution (i.e., without seasonal variation). The PBL height at each grid point is assigned the annual mean height at that grid point. The CO_2 flux from the Biome-BGC model has seasonal variation as in the reference case.

[21] The annual zonal mean CO_2 concentration at the surface produced with constant PBL is shown in Figure 2 along with the reference case for comparison. It shows that the north–south gradient is smaller compared to the reference case. The magnitude of the pole to pole difference is about 2.5 ppm and the IHED is 1.38 ppm. In the absence of covariation between PBL height and CO_2 flux, the pole to pole difference has been reduced by about 30% and the IHED has been reduced by 45%. This result confirms that PBL height and CO_2 flux covariation does contribute to the annual mean latitudinal gradient of CO_2 concentration (mostly over the biospheric source region), but it does not appear to be the dominant mechanism.

[22] In addition to the strong vertical mixing occurring within the PBL, another vertical mixing process is atmospheric convection. Convection is mainly associated with synoptic systems and their frontal structures. Therefore convection may be considered as an integral part of the LSE transport (examined in a following experiment). However, as a sensitivity test, an experiment with convective adjustment turned off in addition to setting the PBL time invariant (the strong mixing within the PBL unchanged) was performed. The biospheric flux has the normal seasonal variation. The resultant zonal mean surface CO_2 concentration gradient is shown in Figure 2. The pole-to-pole difference is now reduced to approximately 1.8 ppm and IHED is 1.10 ppm. This is about a 50% reduction in the pole-to-pole difference and 66% reduction in IHED compared to the reference case. By comparing to the constant PBL case with convection, the covariation of convection and flux appears to contribute about 20% to the north–south annual mean zonal gradient of atmospheric CO_2. The different contributions are not simply additive. Since as noted above, convection is an integral part of the LSE transport.

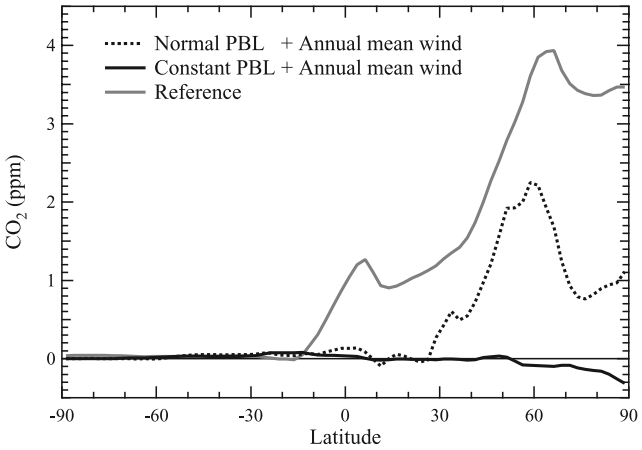

Figure 3. Latitudinal distributions of annual zonal mean surface CO_2 concentrations (in ppm) for two experimental cases: (1) experiment with constant wind (wind field has fixed annual mean values) and (2) experiment with constant wind and constant PBL. The reference case is also shown for comparison.

3.3. Annual Mean Wind Case

[23] To further characterize the role of PBL and flux covariation on the north–south annual mean zonal gradient of atmospheric CO_2, two more experiments were performed to represent the mean wind by fixing the wind field to the 10-year averaged wind field. Thus wind is constant and convection is constant over the 10-year simulation period. Two versions of PBL variations were examined. In one case, the PBL has the normal seasonal variation. The alternate is the constant PBL case, the PBL is fixed at each grid point to its annual mean value (same as the previous experiment). The biospheric flux has the normal seasonal variation in both experiments.

[24] The results of the two experiments are shown in Figure 3. The pole-to-pole CO_2 difference for the normal PBL case is about 1 ppm and IHED is 1.14 ppm. This result shows that the PBL-flux covariation together with the imposed constraint of annual mean atmospheric circulation can produce about 30% of the pole-to-pole difference and 46% of IHED compared to the reference case. These estimates are similar to the estimates from the constant PBL case, section 3.2. This indicates that although the PBL-flux covariation is strong over the land vegetation source regions, the meridional transport required to produce the overall north–south gradient is weak when restricted to the mean circulation. It is consistent with the fact that the midlatitude circulation, the thermally indirect Ferrell cell, is weak. It suggests that the anomaly (LSE) transport is important in the formation of the surface CO_2 gradient.

[25] For the case of the annual mean wind and constant PBL with seasonal variation in the biospheric flux only, there is no transport-flux covariation as the transport in the model is completely constant, and therefore there should be no north–south CO_2 gradient. There is a small possible effect from transport as a result of the mass conservation adjustment for a tracer. The resultant annual zonal mean surface CO_2 concentration has no significant north–south gradient as expected (Figure 3). This null result implies that the pole-to-pole CO_2 difference of approximately 2.5 ppm and IHED of 1.38 ppm for the constant PBL and normal wind simulation (Figure 2) discussed in section 3.2 is mainly due to the covariation of the LSE transport and biospheric flux. This covariation of the LSE transport and flux is a significant rectification mechanism, accounting for more than 50% compared to the reference case in this model, consistent with the result above.

[26] To further compare the reference case, constant PBL case and annual mean wind case (with normal PBL variation), the annual mean spatial distributions of the surface CO_2 concentration for these cases are presented in Figure 4. The reference case shows two main regions of high surface annual mean concentration, the maximum is over 5 ppm.

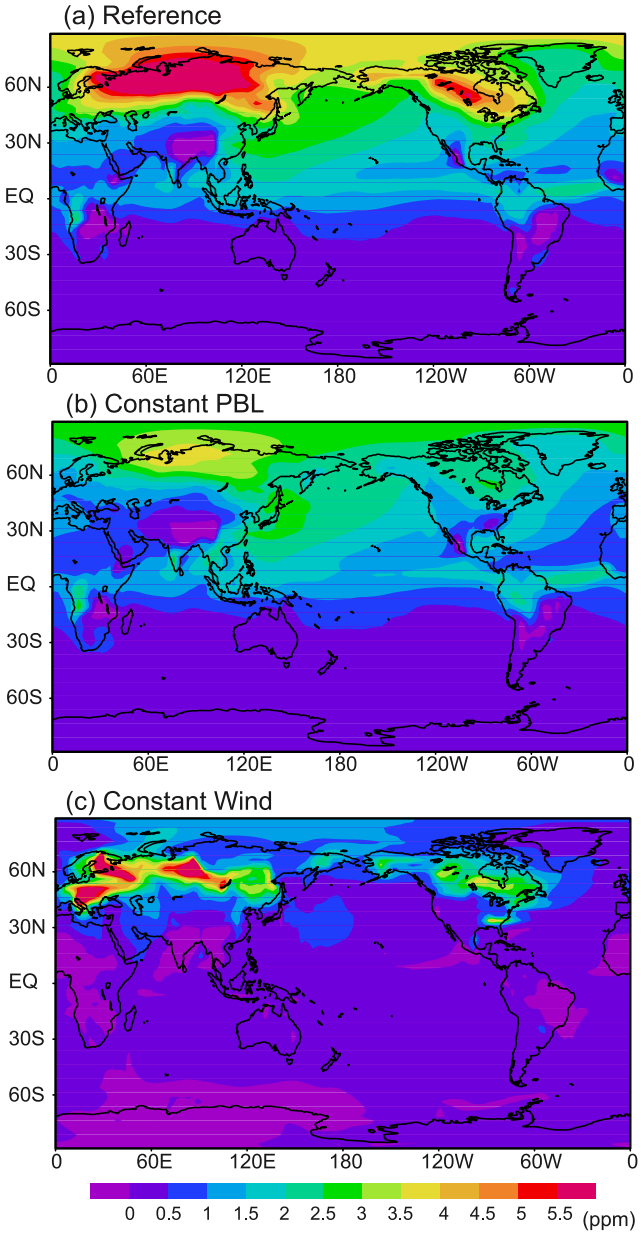

Figure 4. Global distributions of annual mean surface CO_2 concentrations (in ppm) for three experimental cases: (a) reference case, (b) experiment with constant PBL, and (c) experiment with constant wind.

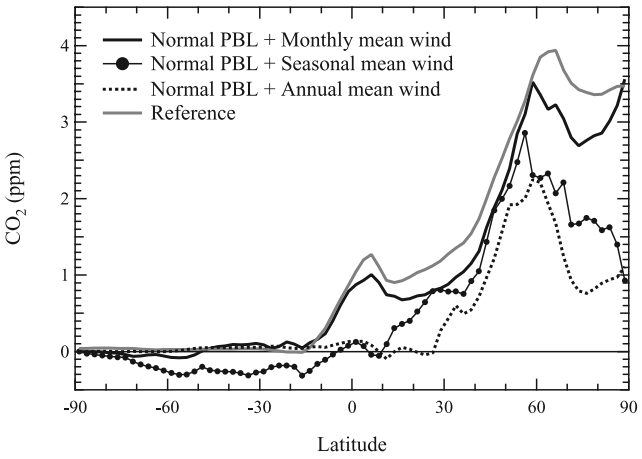

Figure 5. Latitudinal distributions of annual zonal mean surface CO_2 concentrations (in ppm) for two experimental cases: (1) experiment with monthly mean wind and (2) experiment with seasonal mean wind, also shown in the figure are the reference case and the case with annual mean wind (from Figure 3) for comparison.

One large region extends from northeastern Europe to north central Asia (over a large area of Russia), and a smaller region over north-central part of North America (central Canada). These high concentration regions over high latitude land regions give rise to the maximum at $\sim 60^\circ - 70^\circ$N evident in the zonal mean annual surface CO_2 concentration (Figure 2). The north polar region also shows high concentration (up to 4 ppm). Since there are no local flux in the polar region, the high CO_2 concentration is mainly from meridional transport and flux covariation as discussed. The full transport process ensures that the high concentration are dispersed, resulting in the noted mean north–south gradient.

[27] The constant PBL case shows a qualitatively similar picture. The notable difference is over the continental regions in the Northern Hemisphere extratropics. Away from the land regions, the north–south gradient is slightly reduced in magnitude but the spatial pattern is quite similar to the reference case.

[28] The annual mean wind case with normal PBL variation shows quite different results. There are 3 or 4 distinct regions of high annual mean CO_2 concentration (maxima $\sim$5 ppm) over Europe and Russia and a much smaller and weaker high concentration region in central Canada compared to the reference case. These high concentration regions may be interpreted as areas of strong PBL-flux covariation in this model. Thus in this model, North America has only limited areas where the covariation of PBL mixing and flux is strong. The annual mean wind appears to disperse poorly the regions of high concentration, leaving the nonhomogeneous spatial pattern of annual mean surface CO_2 concentration. Consequently the north–south gradient pattern over the ocean regions is relatively weak compared to the reference case and constant PBL case.

[29] In variation to the annual mean wind case, we examined also the roles of seasonal mean wind and monthly mean wind. The monthly mean wind field for each month is obtained by averaging the wind field for that month and also averaging over the 10-year simulation period (there is no interannual variation in the monthly wind in the 10-year simulation period). The seasonal mean winds are 3-month averages for the periods of December–January–February, March–April–May, June–July–August, and September–October–November.

[30] In these two simulations with monthly mean winds and seasonal mean winds, the PBL has the normal seasonal variation. The resultant zonal mean surface CO_2 concentrations are compared in Figure 5. The monthly mean wind case is quite similar to the reference case. The reason is that monthly mean wind (even after the additional 10-year averaging) has retained significant LSE characteristics with month to month variations and anomaly patterns with horizontal length scale $\sim$1000 km. Hence previous LSE analyses [e.g., *Green*, 1970; *Stone*, 1974] have used the annual mean wind as the reference.

[31] The seasonal mean wind case shows a zonal mean surface CO_2 concentration gradient similar to the annual mean wind case. A notable feature is the absence of the small equatorial maximum compared to the monthly mean wind case and reference case, even though the seasonal mean wind retains the movement of the intertropical convergence zone. This tropical region maximum appears to require the shorter timescale transport and flux covariation.

[32] The following sections present the results of more case studies to characterize the sensitivity of the annual mean latitudinal surface CO_2 distribution to the different transport-flux covariations. Although these cases do not represent normal conditions or subsets of normal conditions, they do serve to test the sensitivity of the various transport processes.

3.4. PBL Shifted Case

[33] To study the sensitivity of the north–south annual mean zonal gradient of atmospheric CO_2 to a shift in the PBL-flux covariation, a simulation was performed with the specified monthly PBL height shifted by 6 months. This creates a model condition in which the PBL is shallower in the summer than in the winter. The CO_2 flux and NCEP meteorology in the transport model remain the same as the reference case. In this case, the covariation of PBL height and CO_2 flux is approximately the negative of the reference case.

[34] The annual mean latitudinal surface CO_2 concentration is shown in Figure 6. The PBL and CO_2 flux covariation has a significant effect in the northern midlatitude regions (over the biospheric flux region). The zonal mean concentration has a minimum at $\sim 60^\circ$N of -0.3 ppm. Therefore the photosynthetic removal of CO_2 from a shallow PBL layer in the summer produces very low CO_2 concentration over the land biospheric flux regions. However the weak summer transport does *not* propagate this low CO_2 signal to the northern polar region sufficiently to produce a lower annual mean CO_2 concentration in the northern polar region relative to the tropics. This result indicates that the approximate negation of the covariation of the PBL height and CO_2 flux alone does not result in a negative north–south annual mean zonal gradient of atmospheric CO_2. Hence this covariation does not appear to be the main rectifier mechanism, consistent with previous numerical experiment results. These results are similar to *Law and Rayner* [1999], they noted that shifting all vertical

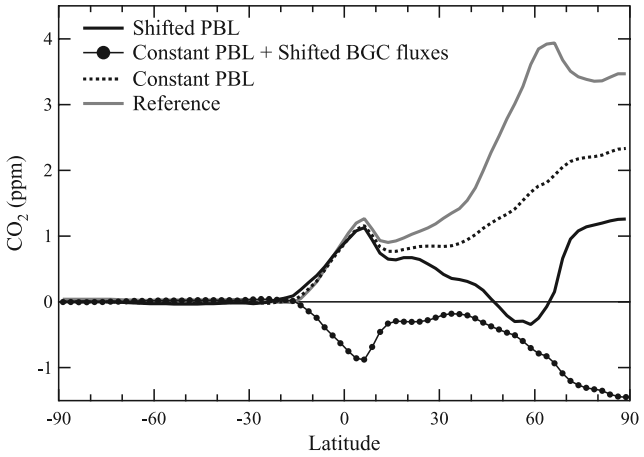

Figure 6. Latitudinal distribution of annual zonal mean surface CO_2 concentration (in ppm) for the experimental cases: (1) experiment with the seasonal variation of PBL height shifted by 6 months (atmospheric wind and biospheric fluxes vary normally) and (2) experiment with the seasonal variation of biospheric fluxes shifted by 6 months and constant PBL (atmospheric wind varies normally), also shown in the figure are the reference case and the case with constant PBL and normal biospheric fluxes (from Figure 2) for comparison.

subgrid scale processes by 6 months has largest impact in the 40–70°N region.

3.5. CO_2 Flux Shifted Case

[35] To examine the robustness of the seasonal covariation of the meridional transport and CO_2 flux, a simulation is performed with the CO_2 flux emission shifted by 6 months (equivalent to shifting the advective and convective transport by 6 months). To focus on this covariation, the PBL is fixed to the annual mean height at each grid point in this simulation, same as the "constant PBL case".

[36] The annual mean latitudinal CO_2 concentration at the surface is shown in Figure 6. The 6-month shift has altered the transport-flux covariation, resulting in a negative CO_2 latitudinal gradient with the minimum CO_2 concentration at the North Pole of $\sim$−1.5 ppm. The negative zonal annual mean gradient is smaller than the positive gradient in the constant PBL case due to the asymmetry in the photosynthetic uptake and respiration CO_2 fluxes. The asymmetry can be seen in the latitude-time plot of the zonal mean NEE flux, Figure 7. The dominant flux pattern in the northern midlatitude shows a strong photosynthetic uptake with a sharp minimum in NEE in June compared to the soil respiration with the broad maximum from November to March.

[37] Any gradient in a conservative tracer field gradually dissipates as a result of advection and diffusion in the atmosphere. Therefore a persistent annual mean north–south CO_2 gradient represents a balance between the transport-flux covariation's preferential transport of higher CO_2 concentration air to the northern polar region from the midlatitude biospheric flux region and the southward dissipation of the steady state gradient. Thus atmospheric dissipation is an important component in the correct modeling of the north–south CO_2 gradient. This dissipation process also determines the north–south CO_2 gradient resulting from fossil fuel CO_2 emission and the net oceanic CO_2 fluxes. Hence atmospheric dissipation has a significant role in the determination of the overall CO_2 distribution from all the CO_2 sources.

4. Conclusions

[38] The covariation of the atmospheric transport and the neutral biospheric CO_2 flux is manifested in atmospheric transport models as a non uniform annual mean CO_2 surface concentration distribution, generally referred to as the rectifier effect. A notable feature in this distribution is a zonal latitudinal gradient with higher concentration at the north polar region compared to the tropics and Southern Hemisphere.

[39] In this study, the NIES atmospheric transport model and the CO_2 flux from the Biome-BGC biospheric model are used to examine the covariation of the different transport mechanisms and the CO_2 flux. The transport mechanisms studied are vertical mixing processes such as the seasonal variation of PBL mixing and convective adjustment, and global atmospheric transport such as the mean meridional circulation and anomaly transport. The results reveal that the annual mean zonal latitudinal gradient of surface CO_2 concentration is the combination of different transport-flux covariation processes.

[40] The reference simulation of the NIES transport model driven by the NCEP reanalysis wind and Biome-BGC fluxes produces an annual zonal mean surface CO_2 distribution with a pole to pole concentration difference of 3.5 ppm (a measure more representative of marine boundary layer condition) and interhemispheric extratropical difference of 2.5 ppm (a measure integrating ocean and land conditions). The main contribution to this north–south CO_2 concentration gradient in this model is the covariation of the LSE transport and the biospheric flux. In the absence of the PBL seasonal variation (the constant PBL case), the

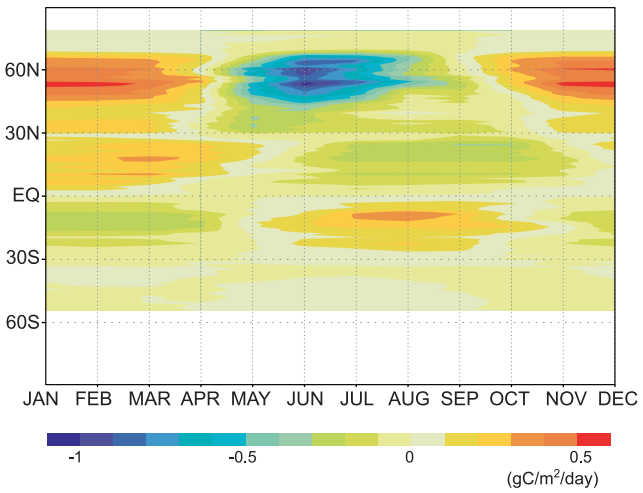

Figure 7. Contour plots of latitudinal and time distribution of the monthly and zonal mean NEE flux from Biome-BGC model. Unit is gCm^{-2} day^{-1}, positive means a CO_2 source for the atmosphere.

model produces a latitudinal CO_2 gradient with a pole to pole difference of about 2.5 ppm (about 70% of the reference case) and interhemisphere extratropical difference of 1.38 ppm (about 55% of the reference case).

[41] The main physical mechanism of the covariation of meridional LSE transport and the biospheric CO_2 flux has the stronger meridional LSE transport associated with higher CO_2 concentration from soil respiration in the winter, and the weaker LSE transport with lower CO_2 concentration from photosynthetic uptake in the summer. The net result of the covariation of the LSE transport and the CO_2 flux is a higher annual mean CO_2 concentration in the northern polar region. The covariation of the seasonal PBL mixing and the CO_2 flux contributes about 30% to the pole to pole difference and about 45% to the interhemispheric extratropical difference simulated in the reference case by the NIES-Biome-BGC model. The results of the various numerical sensitivity experiments conducted in this study indicate that the proportional contributions from the LSE transport-CO_2 flux covariation and the PBL-CO_2 flux covariation to the north–south CO_2 gradient are relatively robust in the NIES transport model.

[42] The relationship among the various components of the transport flux covariation may be summarized as follows. The full transport in the NIES model includes annual mean wind, large-scale eddies, PBL mixing, convection, and vertical subgrid scale mixing. The spatial scale of transport-flux covariation is dependent on the components of transport included. For PBL mixing alone and flux covariation, spatial scale would be at the local point up to the height of the PBL. However, if there are other transport processes included, then PBL-flux covariation acquires the spatial scale from the other transport processes. Thus including LSE transport and PBL variations, the PBL-flux covariation can influence a large area of the extratropics, including the polar region (in this case, PBL-flux covariation may be strongly modulated by the interaction of the biosphere and LSE processes [*Chan et al.*, 2004]). Conversely, the covariation of LSE transport alone (with constant PBL) and flux can account for a significant amount of annual mean CO_2 spatial gradient. The temporal scale of covariation is at least 1 year, since the flux has an annual cycle.

[43] **Acknowledgments.** We would like to thank D. Worthy of Atmospheric Science and Technology Directorate (ASTD), Environment Canada, for providing the CO_2 concentration measurement data. We are grateful to A. Shashkov and R. Staebler of ASTD and the anonymous reviewers for their reviews and comments on the manuscript. This research was supported by a research grant from the Canadian Foundation of Climate and Atmospheric Sciences.

References

Baker, D. F., et al. (2006), TransCom3 inversion intercomparison: Impact of transport model error on the interannual variability of regional CO_2 fluxes, 1988–2003, *Global Biogeochem. Cycles*, *20*, GB1002, doi:10.1029/2004GB002439.

Bakwin, P. S., K. J. Davis, C. Yi, S. C. Wofsy, J. W. Munger, L. Haszpra, and Z. Barcza (2004), Regional carbon dioxide fluxes from mixing ratio data, *Tellus*, *56B*, 301–311.

Chan, D., C. W. Yuen, K. Higuchi, A. Shashkov, J. Liu, J. Chen, and D. Worthy (2004), On the CO_2 exchange between the atmosphere and the biosphere: The role of synoptic and mesoscale processes, *Tellus*, *56B*, 194–212.

Dargaville, R., S. Doney, and I. Y. Fung (2003), Inter-annual variability in the interhemispheric atmospheric CO_2 gradient: Contributions from transport and the seasonal rectifier, *Tellus*, *55B*(2), 711–722.

Deng, F., J. M. Chen, M. Ishizawa, C.-W. Yuen, G. Mo, K. Higuchi, D. Chan, and S. Maksyutov (2007), Global monthly CO_2 flux inversion with a focus over North America, *Tellus*, *59B*(2), 179–190.

Denning, A. S., I. Fung, and D. Randall (1995), Latitudinal gradient of atmospheric CO_2 due to seasonal exchange with land biota, *Nature*, *376*, 240–243.

Denning, A. S., T. Takahashi, and P. Freidlingstein (1999), Can a strong atmospheric CO_2 rectifier effect be reconciled with a "reasonable" carbon budget?, *Tellus*, *51B*, 249–253.

Engelen, R. J., A. S. Denning, K. R. Gurney, and TransCom3 Modelers (2002), On error estimation in atmospheric CO_2 inversions, *J. Geophys. Res.*, *107*(D22), 4635, doi:10.1029/2002JD002195.

Fan, S., M. Gloor, J. Mahlman, S. Pacala, J. Sarmiento, T. Takahashi, and P. Tans (1998), A large terrestrial carbon sink in North America implied by atmospheric and oceanic carbon dioxide data and models, *Science*, *282*, 442–446.

Fujita, D., M. Ishizawa, S. Maksyutov, P. Thornton, T. Saeki, and T. Nakazawa (2003), Inter-annual variability of the atmospheric carbon dioxide concentrations as simulated with global terrestrial biosphere models and atmospheric transport model, *Tellus*, *55B*, 530–546.

Gerbig, C., J. C. Lin, J. W. Munger, and S. C. Wofsy (2006), What can tracer observations in the continental boundary layer tell us about surface-atmosphere fluxes?, *Atmos. Chem. Phys.*, *6*, 539–554.

Green, J. S. A. (1970), Transfer properties of the large-scale eddies and the general circulation of the atmosphere, *Q. J. Royal Meteorol. Soc.*, *96*, 157–185.

Gurney, K., R. Law, P. Rayner, and A. S. Denning (2000), TransCom 3 Experimental Protocol, *Rep., 707*, 93 pp., Dep. of Atmos., Colo. State Univ., Fort Collins, Colo.

Gurney, K. R., et al. (2002), Towards robust regional estimates of CO_2 sources and sinks using atmospheric transport models, *Nature*, *415*, 626–630.

Gurney, K. R., et al. (2003), TransCom 3 CO_2 inversion intercomparision: I. Annual mean control results and sensitivity to transport and prior flux information, *Tellus*, *55B*, 555–579.

Gurney, K. R., et al. (2004), Transcom 3 inversion intercomparison: Model mean results for the estimation of seasonal carbon sources and sinks, *Global Biogeochem. Cycles*, *18*, GB1010, doi:10.1029/2003GB002111.

Gurney, K. R., Y.-H. Chen, T. Maki, S. R. Kawa, A. Andrews, and Z. Zhu (2005), Sensitivity of atmospheric CO_2 inversions to seasonal and interannual variations in fossil fuel emissions, *J. Geophys. Res.*, *110*, D10308, doi:10.1029/2004JD005373.

Higuchi, K., D. Worthy, D. Chan, and A. Shashkov (2003), Regional source/sink impact on the diurnal, seasonal and inter-annual variations in atmospheric CO_2 at a boreal forest site in Canada, *Tellus*, *55B*, 115–125.

Holton, J. R. (2004), *An Introduction to Dynamic Meteorology*, 4th ed., 535 pp., Acad. Press, New York.

Hurwitz, M. D., D. M. Ricciuto, P. S. Bakwin, K. J. Davis, W. Wang, C. Yi, and M. P. Butler (2004), Transport of carbon dioxide in the presence of storm systems over a northern Wisconsin forest, *J. Atmos. Sci.*, *61*, 607–618.

Ishizawa, M., D. Chan, K. Higuchi, S. Maksyutov, C.-W. Yuen, and J. Chen (2006), Rectifier effect in an atmospheric model with daily biospheric fluxes: Impact on inversion calculation, *Tellus*, *58B*(5), 447–462.

Kalnay, E., et al. (1996), The NCEP/NCAR 40-year reanalysis project, *Bull. Am. Meteorol. Soc.*, *77*, 437–471.

Law, R., and P. Rayner (1999), Impacts of seasonal covariance on CO_2 inversions, *Global Biogeochem. Cycles*, *13*, 845–856.

Lin, J. C., C. Gerbig, S. C. Wofsy, A. E. Andrews, B. C. Daube, C. A. Grainger, B. B. Stephens, P. S. Bakwin, and D. Y. Hollinger (2004), Measuring fluxes of trace gases at regional scales by Lagrangian observations: Application to the CO_2 Budget and Rectification Airborne (COBRA) study, *J. Geophys. Res.*, *109*, D15304, doi:10.1029/2004JD004754.

Maksyutov, S., and G. Inoue (2000), Vertical profiles of radon and CO_2 simulated by the global atmospheric transport model, in *CGER Supercomputer Activity Report*, *I039-2000, 7*, edited by H. Shimizu, pp. 39–41, CGER NIES, Tsukuba, Japan.

Peixoto, J. P., and A. Oort (1992), *Physics of Climate*, 520 pp., Am. Inst. of Phys., New York.

Randerson, J. T., M. V. Matthew, T. J. Conway, I. Y. Fung, and C. B. Field (1997), The contribution of terrestrial sources and sinks to trends in the seasonal cycles of atmospheric carbon dioxide, *Global Biogeochem. Cycles*, *11*, 553–560.

Stone, P. H. (1974), The meridional variation of the eddy heat fluxes by baroclinic waves and their parameterization, *J. Atmos. Sci.*, *31*, 444–456.

Taguchi, S. (1996), A three-dimensional model of atmospheric CO_2 transport based on analyzed winds: Model description and simulation results for TRANSCOM, *J. Geophys. Res.*, *101*, 15,099–15,109.

Taylor, J. A. (1998), Atmospheric mixing and the CO_2 seasonal cycle, *Geophys. Res. Lett.*, *25*, 4173–4176.

Thornton, P. E., et al. (2002), Modeling and measuring the effects of disturbance history and climate on carbon and water budgets in evergreen needleleaf forests, *Agric. For. Meteorol.*, *113*, 185–222.

Trivett, N. B. A., and K. Higuchi (1989), Trends and seasonal cycles of atmospheric CO_2 over Alert, Sable Island, and Cape St. James, as analyzed by forward stepwise regression technique, in *The Statistical Treatment of CO_2 Data Records*, edited by W. P. Elliott, pp. 27–42, Air Resources Laboratory, Silver Spring, Md.

Worthy, D E. J., A. Platt, R. Kessler, M. Ernst, and S. Racki (2003), The greenhouse gases measurement program, measurement procedures and data quality, in *Canadian Baseline Program; Summary of Progress to 2002*, edited by D. Worthy, pp. 97–120, Meteorological Service of Canada, Toronto.

Yi, C., K. J. Davis, B. W. Berger, and P. S. Bakwin (2001), Long-term observations of the dynamics of the continental planetary boundary layer, *J. Atmos. Sci.*, *58*, 1288–1299.

Yi, C., K. J. Davis, P. S. Bakwin, A. S. Denning, N. Zhang, A. Desai, J. C. Lin, and C. Gerbig (2004), The observed covariance between ecosystem carbon exchange and atmospheric boundary layer dynamics at a site in northern Wisconsin, *J. Geophys. Res.*, *109*, D08302, doi:10.1029/2003JD004164.

D. Chan, K. Higuchi, and M. Ishizawa, Atmosheric Science and Technology Directorate, Environment Canada, 4905 Dufferin Street, Toronto, ON, Canada M3H 5T4. (douglas.chan@ec.gc.ca)

J. Chen, Department of Geography, University of Toronto, 62 St. George Street, Toronto, ON, Canada M5S 3G3.

S. Maksyutov, National Institute for Environmental Studies, 16-2 Onogawa, Tsukuba 305-8506, Japan.